Tensile properties of Si nanowires with faulted stacking layers

Haifei Zhan, Yuantong Gu*, Cheng Yan and Prasad K.D.V. Yarlagadda

School of Chemistry, Physics and Mechanical Engineering, Queensland University of Technology, Brisbane, 4001, QLD, Australia
(Received Nov 1 2012, accepted Dec 9 2013)

Semiconductor nanowires (NWs) show tremendous applications in micro/nano-electro-mechanical systems. In order to fulfill their promising applications, an understanding of the mechanical properties of NWs becomes increasingly important. Based on the large-scale molecular dynamics simulations, this work investigated the tensile properties of Si NWs with different faulted stacking layers. Different faulted stacking layers were introduced around the centre of the NW by the insertion or removal of certain stacking layers, inducing twins, intrinsic stacking fault, extrinsic stacking fault, and 9R structure. Stress-strain curves obtained from the tensile deformation tests reveal that the presence of faulted stacking layers has induced a considerable decrease to the yield strength while only a minor decrease to Young's modulus. The brittle fracture phenomenon is observed for all tested NWs. In particular, the formation of a monatomic chain is observed for the perfect NW, which exists for a relatively wide strain range. For the defected NW, the monatomic chain appears and lasts shorter. Additionally, all defected NWs show a fracture area near the two ends, in contrast to the perfect NW whose fracture area is adjacent to the middle. This study shed lights on the better understanding of the mechanical properties of Si NWs with the presence of different faulted stacking layers.

Keywords: tensile, nanowire, stacking faults, fracture, monatomic chain, molecular dynamics simulation

1. INTRODUCTION

Metal and semiconductor nanowires (NWs) show tremendous technological applications in micro/nano-electro-mechanical systems (MEMS and NEMS), such as high frequency resonators[1], field effect transistors (FETs)[2], nano switches[3], actuators[4] and others. Therefore, investigation of the mechanical properties of NWs, which is crucial to realize the full potentials of NWs, has attracted intensive research interests in recent years, in terms of experimental, theoretical and numerical studies. On the experimental front, researchers have developed/established different in situ testing approaches to characterize NWs. For instance, Zhu et al.[5] conducted an investigation of the Young's modulus and fracture strength of Si NWs with diameters between 15 and 60 nm and length ranging from 1.5 to 4.3 μm. The fracture strength of [111] Si NW[6] and the elastic modulus of ZnO NWs[7, 8] subjected to bending was measured. On the theoretical front, most researchers have utilized surface-based extensions of continuum elasticity theory[9, 10] to examine surface stress effects on the mechanical properties of NWs. Large volume of numerical studies including multi-scale simulations[11-13], molecular dynamics (MD) simulations have been reported. Specifically, the mechanical properties or behaviors under a wide range of loading conditions including tension[14], compression[15], bending[16], torsion[17] and vibration[18, 19] have been studied.

* School of Chemistry, Physics and Mechanical Engineering, Queensland University of Technology, Brisbane 4001, Australia. Email: yuantong.gu@qut.edu.au

It is noticed that majority of previous studies have focused on NWs with perfect crystal structures owing to the decreased possibility of defects and flaws in NWs. However, recent experimental studies reveal that NWs also contain certain defects. For instance, metal NWs are found usually polycrystalline, containing grain boundaries (GBs) that transect the whole NW normal to its longitudinal axis into a bamboo structure[20]. Lopez et al.[21] reported the existence of ordered stacking fault arrays in Si NWs, and (001) stacking defects are also observed to intersperse with small cubic GaN regions in the GaN NW[22]. Researchers demonstrated that, the controlling of twinning and polytype generation in III-V NW systems, allowing for pure wurtzite and zinc-blended NWs to be grown[23]. Davidson et al.[24] reported the occurrence of twinning planes along the growth axis of <112> oriented Si NWs, which, for instance, produces a local hexagonal ordering of ABA regarding with the perfect stacking sequence of ABC along a <111> direction. Hence, it is of great scientific interests to study the influences of different defects on the mechanical performance of NWs. Relevant research is still rare in the literature.

In this work, large-scale MD simulations will be employed to investigate the mechanical properties of Si NWs with faulted stacking layers, including the existences of twins, intrinsic stacking faults, extrinsic stacking faults and others. Focus will be paid to the effects of different stacking faults on the Young's modulus, yield strength and deformation behaviors of NWs.

2. COMPUTATIONAL DETAILS

Large-scale MD simulations were carried out on <112> orientated Si NWs with different kinds of faulted stacking layers. Fig. 1 illustrated the crystal structure of Si NWs with a circular cross-section that being studied. As is known, for the perfect diamond structure, the stacking sequence of the {111} planes is *AaBbCc*, which is described by the simple sequence *ABC* as shown in Fig. 1b. In this work, the low-energy faults such as twins and stacking faults in Si NWs were considered, which involve no change in the four nearest-neighbor covalent bonds in the lattice. Different faulted stacking layers were introduced around the centre of the NW by insertion or removal of certain stacking layers[25], inducing twins (stacking sequence of ABCACBA in Fig. 1c), intrinsic stacking fault (stacking sequence of ABCBCAB in Fig. 1d), extrinsic stacking fault (stacking sequence of ABCABAC in Fig. 1e), and 9R structure (stacking sequence of ABCBCAC in Fig. 1f). The 9R structure is constructed based on the recent experimental work by Lopez et al.[21]. These defected NWs are referred as NW-TB, NW-iSF, NW-eSF and NW-9R for discussion simplicity, respectively.

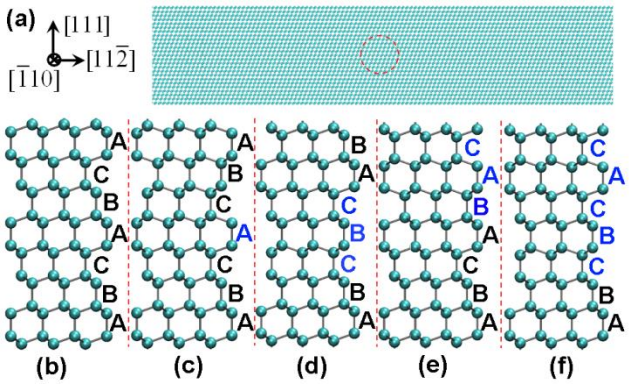

Fig. 1 Crystal structure of <112> orientated Si NWs with different kinds of faulted stacking layers. (a) A snapshot of the cross-section view of the NW along axis; (b) Perfect ABC stacking sequence; (c) Stacking sequence of twins; (d) Stacking sequence of an intrinsic stacking fault; (e) Stacking sequence of an extrinsic stacking fault; (f) Stacking sequence of the 9R structure.

In general, five NWs were studied with an identical radius of 4 nm, and a length of 80 nm. The SW many body potential[26] was adopted to describe the Si atomic interaction, which allows realistic surface reconstruction. To monitor the deformation process, the coordinate number has been applied to distinguish atoms from perfect and deformed crystal structures. During each simulation, the NW was first relaxed to a minimum energy state using the conjugate gradient algorithm, e.g., the length of the NW was allowed to decrease in response to the tensile surface stress. After that, the NW was equilibrated at 10 K for 400 picoseconds at a time step of 1 fs using Nose-Hoover thermostat[27, 28] (NPT ensemble). Finally, the NW was elongated by applying a constant strain rate along the *z*-direction. Periodic boundary conditions were utilized along the longitudinal direction of the NW. All simulations were performed using the open-source LAMMPS code developed at Sandia National Laboratories[29]. In addition, Young's modulus is determined directly from the stress-strain curve with the strain <3% using linear regression. According to the continuum mechanics and the atomic configurations, yield strength is referred as the stress when plastic deformation (e.g. partial dislocations or cracks) first emitted or the NW is fractured, and the corresponding strain is taken as yield strain. Specifically, the engineering strain is used in this work, which is defined as $\varepsilon = (l - l_0)/l_0$, here, l is the instantaneous length and l_0 is the initial length of the NW after the relaxation under NPT ensemble.

3. RESULTS AND DISCUSSSION

3.1 Perfect <112> Si NW

We first investigated the tensile properties of perfect <112> orientated Si NW. Figure 2 shows the stress-strain curve obtained during the tensile test. Basically, the stress is ob-

served to increase almost linearly at the beginning of elongation. After a period of loading, the maximum stress is achieved, followed by a sudden drop. Particularly, as seen in Fig. 2a, the stress is almost directly reduced to and saturated around 0 GPa after passing the maximum value. According to the corresponding atomic configurations, the Si NW retains their initial crystal structure before the peak stress, i.e., the NW is under elastic deformation as illustrated in Fig. 2b. The peak stress is regarded as the yield strength of the NW, which is estimated around 15.124 GPa corresponding to the strain of 0.157. It is observed that, cracks begin to initiate when the stress is approaching the yield strength (see Fig. 2c), and quickly propagate through the entire cross-section of the NW, eventually led to the fracture of the NW, as shown in Fig. 2d.

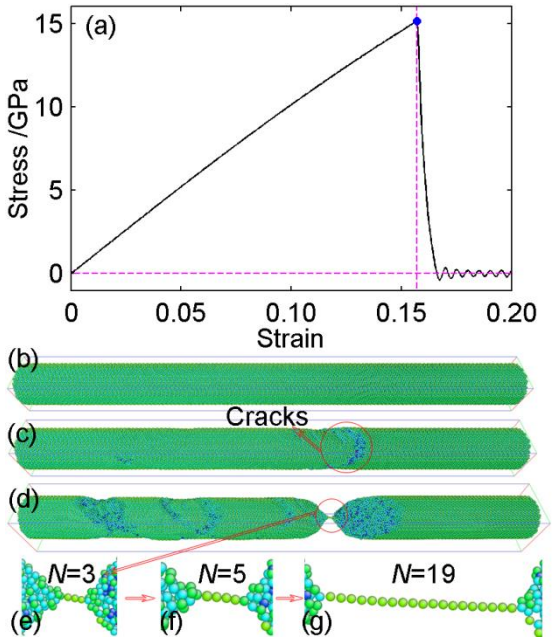

Fig. 2 Tensile testing results for the perfect <112> orientated Si NW. (a) Stress-strain curve; Atomic configuration at the strain of: (b) 0.156; (c) 0.158. (d) 0.168; Monatomic chain at the strain of: (e) 0.168. (f) 0.172. (g) 0.222. Atomic configurations are visualized according the coordination numbers ranging from 0 to 8.

The most striking observation is that, a monatomic strain is formed after fracture, as illustrated in Fig. 2e. Particularly, the length of this chain or atoms number (N) increases with the increase of strain (e.g., N increase from 3 at the strain of 0.168 to 19 at the strain of 0.222 as revealed in Fig. 2g), and finally broke up at the strain of 0.236 (with N=22). It is supposed that the formation of such interesting monatomic strain should be related with several issues, like the crystal orientation, atomic potential, strain rate, temperature and others. This means that a large number of testings are still required to identify its occurrence. However, further investigations on the monatomic strain will not be the aim of this paper.

3.2 Si NW with faulted stacking layers

Fig. 3 reveals the stress-strain curves from all five considered NWs. It is evident that all NWs show a brittle property, i.e., the NW is fractured at certain strain. Basically, before fracture, theses curves share almost same gradient, indicating a similar Young's modulus. On the contrary, the yield strength has received a considerable decrease due to the presence of different faulted stacking layers, together with a significant decrease to the corresponding yield strain.

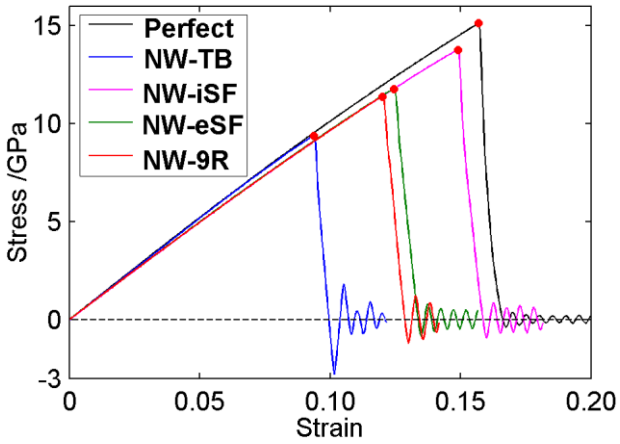

Fig. 3 Stress-strain curves for Si NWs with different faulted stacking layers.

Several atomic configurations have been selected to further depict the deformation process of the NW as presented in Fig. 4. As aforementioned, all NWs exhibit brittle behaviors, i.e., cracks initiate at the yield strain (Figs. 4a1, c, e and g) and quickly propagate to the entire cross-section, leading the facture of the NW (Figs. 4b, d, f and h). The fracture location for all defected NWs is found near the end, while for the perfect NW, the fracture area is adjacent to the middle (see Fig. 2d). Specifically, from Fig. 4a, no obvious fracture area is found from the major body of the NW with one twin boundary, which is due to the fracture area is located around the NW's two ends. As seen in Fig. 4a1, by shifting the entire NW along z-axis (i.e., periodic direction), the fracture area can be easily observed. Since all NWs considered currently have a periodic boundary condition in the axial direction, hence, the necking or fracture locations could be anywhere.

Besides the fracture area, the clear formation of monatomic chain is also observed. Due to the lack of obvious fracture tip, two parallel monatomic chains are identified for the NW with one twin boundary (see inset figure of Fig. 4b). Whereas, for NWs with either intrinsic or extrinsic SFs, a single monatomic chain is developed between the two fracture tips (see inset figures of Figs.4d and f). For NW with a 9R structure, a multiple atomic chain is generated (see Fig. 4h). Generally, it is found that the monatomic chain in the defected NWs is shorter and easier to break up than that in

the perfect NW. More specifically, for the defected NWs, the monatomic chain only sustains for a short period, which in the other hand prevents the formation of longer chains.

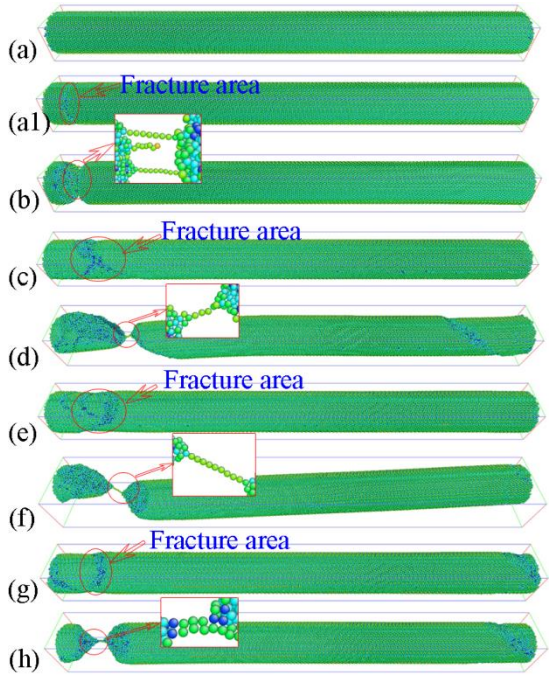

Fig. 4 Atomic configurations of Si NWs at different strain points. NW with one twin boundary at the strain of: (a) 0.094, (a1) 0.094, being shifted along *z*-axis, (b) 0.096, being shifted along *z*-axis; NW with intrinsic stacking faults at the strain of: (c) 0.15, (d) 0.158; NW with extrinsic stacking faults at the strain of: (e) 0.126, (f) 0.15; NW with 9R structure at the strain of: (g) 0.1221, (h) 0.1281. Atomic configurations are visualized according the coordination numbers ranging from 0 to 8.

In all, as summarized in Table I, for the perfect <112> NW, Young's modulus is estimated around 104.96 GPa, with the yield strength as 15.124 GPa. An insignificant decrease of Young's modulus is observed for the defected NWs, whereas, the yield strain and yield strength received an obvious decrease, e.g., about 37.93% reduction of the yield strength is observed for the NW with a twin boundary. It is concluded that different faulted stacking layers have induced an evident influence to the yield strength to the NW, which only exert minor influence to the Young's modulus of NWs.

Table I. Young's modulus (*E*), yield strength (*YS*) and yield strain of different Si NWs as obtained from MD results

	Perfect	TB	iSF	eSF	9R
E (GPa)	104.96	103.22	99.608	100.54	100.41
YS (GPa)	15.124	9.388	13.766	11.779	11.372
Yield strain	0.157	0.094	0.149	0.124	0.120

4. CONCLUSIONS

Based on the large-scale MD simulation, the impacts on the tensile properties of <112> orientated Si NWs from different faulted stacking layers (including twin boundary, intrinsic stacking faults, extrinsic stacking faults and 9R structure) have been explored. The atomic configurations at different strain points have been compared carefully between different NWs. Major conclusions can be drawn as below:

- Both perfect and defected NWs exhibit brittle properties, i.e., all NW are fractured after yielding;
- For the perfect NW, a monatomic chain is formed after yielding, which is observed to grow from a three atoms chain to 22 atoms chain, and sustain for a relatively wide strain range;
- Due to the presence of faulted stacking layers, the yield strength and yield strain have received a considerable decrease;
- Young's modulus appears insensitive to the existence of different faulted stacking layers;
- The formation of the monatomic chain is apparently influenced by the faulted stacking layers, i.e., for defected NWs, the monatomic chain appears shorter and lasts shorter;

In summary, this study provides a first investigation on the tensile properties of Si NWs with faulted stacking layers, which will enhance and extend the current understanding of the mechanical behaviors of NWs, and eventually benefit the fulfillment of the potential applications of NWs.

Acknowledgement: Support from the ARC Future Fellowship grant (FT100100172) and the High Performance Computer resources provided by the Queensland University of Technology are gratefully acknowledged.

References and Notes

1. A. Husain, J. Hone, H. W. C. Postma, X. Huang, T. Drake, M. Barbic, A. Scherer, and M. Roukes, Appl. Phys. Lett. 83, 1240 **(2003)**.
2. R. M. Ma, L. Dai, H. B. Huo, W. J. Xu, and G. Qin, Nano Lett. 7, 3300 **(2007)**.
3. M. Liao, S. Hishita, E. Watanabe, S. Koizumi, and Y. Koide, Adv. Mater. 22, 5393 **(2010)**.
4. Y. Berdichevsky and Y. H. Lo, Adv. Mater 18, 122 **(2006)**.
5. Y. Zhu, F. Xu, Q. Qin, W. Y. Fung, and W. Lu, Nano Lett. 9, 3934 **(2009)**.
6. S. Hoffmann, et al., Nano Lett. 6, 622 **(2006)**.
7. J. Song, X. Wang, E. Riedo, and Z. L. Wang, Nano Lett. 5, 1954 **(2005)**.
8. C. Chen and J. Zhu, Appl. Phys. Lett. 90, 043105 **(2007)**.
9. J. He and C. Lilley, Appl. Phys. Lett. 93, 263108 **(2008)**.
10. G. F. Wang and X. Q. Feng, Appl. Phys. Lett. 90, 231904 **(2007)**.
11. H. S. Park and P. A. Klein, J. Mech. Phys. Solids 56, 3144 **(2008)**.
12. H. S. Park, J. Appl. Phys. 103, 123504 **(2008)**.

13. S. Y. Kim and H. S. Park, Nano Lett. 9, 969 **(2009)**.

14. H. Park, K. Gall, and J. Zimmerman, J. Mech. Phys. Solids 54, 1862 **(2006)**.

15. H. F. Zhan and Y. T. Gu, Editor: Kaneko, Shigehiko, Proceedings of the *14th Asia-Pacific Vibration Conference*, **(2011)** December 5-8,HongKong.

16. H. F. Zhan and Y. T. Gu, Comput. Mater. Sci. 55, 73 **(2012)**.

17. H. F. Zhan, Y. T. Gu, C. Yan, and P. K. D. V. Yarlagadda, Adv. Mat. Res. 335, 498 **(2011)**.

18. H. F. Zhan and Y. T. Gu, J. Appl. Phys. 111, 124303 **(2012)**.

19. H. F. Zhan, Y. T. Gu, and H. S. Park, Nanoscale, 4, 6779 **(2012)**.

20. A. Bietsch and B. Michel, Appl. Phys. Lett. 80, 3346 **(2002)**.

21. F. J. Lopez, E. R. Hemesath, and L. J. Lauhon, Nano Lett. 9, 2774 **(2009)**.

22. D. Tham, C. Y. Nam, and J. E. Fischer, Adv. Funct. Mater. 16, 1197 **(2006)**.

23. R. E. Algra, M. A. Verheijen, M. T. Borgström, L. F. Feiner, G. Immink, W. J. P. van Enckevort, E. Vlieg, and E. P. A. M. Bakkers, Nature 456, 369 **(2008)**.

24. F. M. Davidson III, D. C. Lee, D. D. Fanfair, and B. A. Korgel, J. Phys. Chem C 111, 2929 **(2007)**.

25. J. P. Hirth and J. Lothe, John Wiley and Sons, Inc., 1982, 857 **(1982)**.

26. F. H. Stillinger and T. A. Weber, Phys. Rev. B 31, 5262 **(1985)**.

27. W. G. Hoover, Phys. Rev. A 31, 1695 **(1985)**.

28. S. Nosé J. Chem. Phys. 81, 511 **(1984)**.

29. S. Plimpton, J. Comput. Phys. 117, 1 **(1995)**.